Computer Methods in Biomechanics and Biomedical Engineering
Vol. 00, No. 00, May 2008, 1–14

GUIDE

An optimization approach to multiprobe cryosurgery planning

Giovanni Giorgi[a], Leopoldo Avalle[a], Massimo Brignone[b], Michele Piana[a,c*] and Giacomo Caviglia[a]

[a] *Dipartimento di Matematica, Università di Genova*; [b] *Azienda Ospedaliera Universitaria San Martino, Genova*; [c] *Consiglio Nazionale delle Ricerche CNR - SPIN, Genova*

(*Received 00 Month 200x; final version received 00 Month 200x*)

In cryosurgery operations tumoral cells are killed by means of a freezing procedure realized with insertion of cryoprobes in the diseased tissue. Cryosurgery planning aims at establishing the best values for operation parameters like number and position of the probes or temperature and duration of the freezing process. **Here we present an application of Ant Colony Optimization (ACO) to cryosurgery planning, whereby the ACO cost function is computed by numerically solving several direct Stefan problems for biological tissues.** The method is validated in the case of a 2D phantom of a prostate cross-section.

Keywords: Cryosurgery planning, Euler-Galerkin method, Ant Colony Optimization.

1. Introduction

Cryosurgery is a minimally invasive technique aiming at the destruction of cancerous tissues by application of extremely cold temperatures. It may be used in the treatment of localized prostate and liver carcinomas, in alternative to resection, radiation and chemotherapy **(Cohen 2004; Theodorescu 2004; Zhang et al 2005; Chua and Chou 2009; Shitzer 2011)**.

The cooling and the subsequent destruction of living tissues is performed by insertion of multiple cryoprobes in the shape of long hypodermic needles connected to an external generator of supercooled fluid (Rossi et al 2010). Subtraction of heat from the biological system leads to a phase change from the liquid to the solid state, starting around the tip of the cryprobes. The process is carried on until the entire cancerous tissue is frozen with temperature range of the solid phase below the lethal limit. To obtain an effective destruction of cancerous tissues several freezing-thawing cycles at appropriate temperature variation rates may be required (Chua and Chou 2009). To minimize cryoinjury to the surrounding healthy cells and blood vessels, cryoheaters have also been developed, to be inserted into the tissues (Rabin and Stahovich 2003; Rossi et al 2010).

A reliable mathematical model of cryosurgery operation requires the determination of the spatial distribution and time evolution of the temperature field inside the tissue volume, when heat is subtracted by the cryoprobes and new heat enters the unfrozen subregions of the tissue, as a consequence of blood perfusion and metabolism. Cryoprobes, cryoheaters and healthy tissue around the tumor provide

*Corresponding author. Email:piana@dima.unige.it

ISSN: 1741-5977 print/ISSN 1741-5985 online

DOI: 10.1080/1741597YYxxxxxxxx
http://www.informaworld.com

boundary data for the temperature transient field. Thus the determination of the transient temperature reduces to the solution of a (direct) Stefan problem for a phase change.

Unlike pure substances, biological tissues do not have a fixed freezing point but phase changes are taken to occur over a temperature range, so that between the solid phase and the normal tissue there is an intermediate, time dependent spatial region (Shitzer 2011; Chua and Chou 2009; Rabin and Shitzer 1998). A further complication arises from the fact that analytic solutions of the propagation equation are seldom at disposal and therefore only numerical methods can provide an adequate framework for cryosurgery simulations.

In order to destroy cancerous tissues while preserving the adjacent healthy organs, the design of a cryosurgery operation requires the optimal choice of placements of cryoprobes with the related shapes and dimensions (Keanini and Rubinsky 1992; Rabin and Stahovich 2003; Rabin et al 2004), the most appropriate insertion depth (Rossi et al 2007), the optimal temperature law for the cryoprobes (Baissalov et al 2000). Among the optimization techniques employed we recall the simplex method (Keanini and Rubinsky 1992), the gradient-descent method (Baissalov et al 2001), the force-field analogy (Rossi et al 2010; Tanaka et al 2006), **the bubble-packing method (Rossi et al 2008)**.

In this paper we describe a new systematic procedure to deal with cryosurgery planning based on the application of the Ant Colony Optimization (ACO) method (Socha and Dorigo 2003). The novelty of this approach lies in the generality of its formulation since ACO is independent from the physical interpretation and from the number of the parameters subjected to optimization. In other words, trough ACO, one is able to set different kinds of free planning parameters without changing the optimization technique.

As a first application, here we consider the problem of determining the best location for cryprobes and cryoheaters. **The algorithm is based on an iterative procedure consisting in the solution of several (direct) Stefan problems at each step**. Every step begins with the assumption that the placement of cryoprobes and cryoheaters is given while cryoprobes, cryoheaters, tumor and background tissue are at the temperature of 37 ^{o}C. Next the direct Stefan problem is solved as the temperature of the cryoprobes is lowered down to -145 ^{o}C, until the tumor is almost completely frozen. The resulting temperature field is processed to evaluate **the defect weight function (Lung et al 2004)** providing a quantitative estimate of the mismatch between the frozen tissue at sufficiently low temperature and the tissue to be destroyed. **ACO utilizes this cost functional and yields the new positions of cryoprobes and cryoheaters in order that the next step can begin.** The procedure stops when the further correction of the position of cryoprobes and cryoheaters becomes negligible.

The plan of the paper is as follows. Section II provides a description of the mathematical model for a typical freezing process in a diseased biological tissue. In section III, the numerical method for the solution of the direct Stefan problem is described. Section IV discusses the statistical algorithm utilized for optimizing the operation design. Section V contains some numerical examples including an application of our method to a more sophisticated planning. Finally, our conclusions are offered in Section VI.

2. Mathematical model

The setup of a cryosurgical operation begins by decreasing the temperature of the cryoprobes according to a prescribed law down to a minimum value. The cryoprobes act as heat sinks removing sensible and latent heat from the tumor. The related direct Stefan problem is solved under the following assumptions.

(a) During freezing, heat is moved from the cancerous tissue towards the cryoprobes by conduction. **Inside the volume where phase-change occurs, we take into account the transformation between sensible heat and latent heat.** Local heat supply by blood perfusion and metabolism is also considered until the tissue is frozen. There is no heat supply by radiation.

(b) The cancerous tissue is not regarded as a pure substance. Thus phase change takes place over a temperature range, **where the upper limit θ_M and the lower limit θ_m are differently chosen in the literature, (for example, $\theta_m = -10$, $\theta_M = 0$ in (Zhang et al 2005) and $\theta_m = -8$, $\theta_M = -1$ in (Rabin and Shitzer 1998))**. This means that the formation of ice crystals during freezing begins at θ_M and ends at θ_m; within this temperature interval, both latent heat and sensible heat are removed from the tissue. The temperature interval (θ_m, θ_M) identifies the intermediate region V_2 of the phase change, which is placed between solid and liquid phases. The temperature interval $\theta > \theta_M$ determines the region V_3, filled by tissue-liquid phase, while the condition $\theta < \theta_m$ determines the region V_1, filled by the frozen-solid tissue (see Figure 1).

(c) The material parameters in V_1 and V_3, such as mass density, specific heat capacity, and thermal conductivity are taken as constant. However they are supposed to assume different values inside the frozen and the unfrozen region. Volume changes and the related stress depending on temperature changes are neglected.

(d) The latent heat in the intermediate region V_2 is constant. The latent heat effect is modeled by assuming a suitable heat capacity over the corresponding temperature range (Bonacina et al 1973). The thermal conductivity of the intermediate region is regarded as a function of temperature.

(e) The initial temperature value in the Stefan problem is 37 ^{o}C for the whole tissue. The (boundary) value of the temperature varies according to a prescribed law at the boundary of the cryoprobes while it is fixed at 37 ^{o}C in the surrounding healthy tissue and at the boundary of the cryoheaters.

The heat transfer process is described in terms of the corresponding temperature field $\theta(\mathbf{x}, t)$, where $\mathbf{x}$ is the position vector and t the time. The partial differential equations for the temperature field in the regions V_1, V_2 and V_3 follow from the previous assumptions, as well as the related boundary and initial conditions.

In the unfrozen region, V_3, the temperature θ satisfies the classical heat balance equation for biological tissues (Pennes 1948),

$$\rho_3 \, c_3 \, \frac{\partial \theta}{\partial t} = \nabla \cdot (k_3 \, \nabla \theta) + \omega_b \, \rho_b \, c_b \, (\theta_b - \theta) + q_m. \tag{1}$$

In the frozen region, V_1, equation (1) simplifies to

$$\rho_1 \, c_1 \, \frac{\partial \theta}{\partial t} = \nabla \cdot (k_1 \, \nabla \theta). \tag{2}$$

Subscripts $1, 2, 3$ refer to the corresponding region or phase; b refers to the arterial blood; ρ is the mass density, kg/m^3; c is the specific heat, J /(kg ^{o}C); t is the time, s; k is the thermal conductivity, W/(m ^{o}C); w_b is the capillary blood perfusion

rate, 1/s; θ_b is the blood temperature, ^{o}C; q_m is the metabolic heat generation rate, W/m^3.

Eq. (1) expresses conservation of (thermal) energy in mechanical equilibrium. The three terms at the right hand side of (1) are related to *a*) heat transfer by conduction; *b*) heat supply to the tissue by blood flow, under the assumption that blood enters the capillaries at temperature θ_b; *c*) heat supply as a consequence of chemical reactions inside the cells. Eq. (2) is the classical heat equation in the simplest form, showing that heat transfer inside the frozen region is only due to conduction.

The heat transfer process in the intermediate region V_2 is modeled by approximating latent heat exchange in the interval (θ_m, θ_M) with a predefined heat capacity (Bonacina et al 1973). This is essentially correspondent to an enthalpy formulation, although enthalpy is not explicitly introduced (Bonacina et al 1973), (Zhao et al 2007). The thermal conductivity k is represented by a linear function of θ which is continuous at the boundary of the intermediate region and leads to convenient boundary conditions. Specifically, we let

$$\rho_2\, c_2 := \frac{L}{\theta_M - \theta_m} + \frac{\rho_1\, c_1 + \rho_3\, c_3}{2}, \tag{3}$$

$$k_2(\theta) := k_1 + \frac{k_3 - k_1}{\theta_M - \theta_m}\,(\theta - \theta_m), \tag{4}$$

where L denotes the latent heat per unit volume. In particular we have $k_2(\theta_m) = k_1$ and $k_2(\theta_M) = k_3$. The resulting equation for θ in V_2 takes the form

$$\rho_2\, c_2\, \frac{\partial \theta}{\partial t} = \nabla \cdot (k_2(\theta)\, \nabla\theta) + \omega_b\, \rho_b\, c_b\, (\theta_b - \theta) + q_m. \tag{5}$$

As usual, it is required that the temperature and the normal component of the heat flux vector are continuous at the common boundaries of the three regions. Finally, the temperature is given at the boundary of the cryoprobes and at the external boundary of V_3, where $\theta = 37\ ^o$C. The initial datum is $\theta = 37\ ^o$C everywhere.

Our numeric approach to the direct Stefan problem is based on the following compact formulation. We define

$$a(\theta) := \begin{cases} \rho_1\, c_1 & \text{in } V_1 \\ \rho_2\, c_2 & \text{in } V_2 \\ \rho_3\, c_3 & \text{in } V_3 \end{cases} \tag{6}$$

$$k(\theta) := \begin{cases} k_1 & \text{in } V_1 \\ k_2 & \text{in } V_2 \\ k_3 & \text{in } V_3 \end{cases} \tag{7}$$

$$b(\theta) := \begin{cases} 0 & \text{in } V_1 \\ \omega_b\, \rho_b\, c_b\, (\theta_b - \theta) + q_m & \text{in } V_2 \\ \omega_b\, \rho_b\, c_b\, (\theta_b - \theta) + q_m & \text{in } V_3. \end{cases} \tag{8}$$

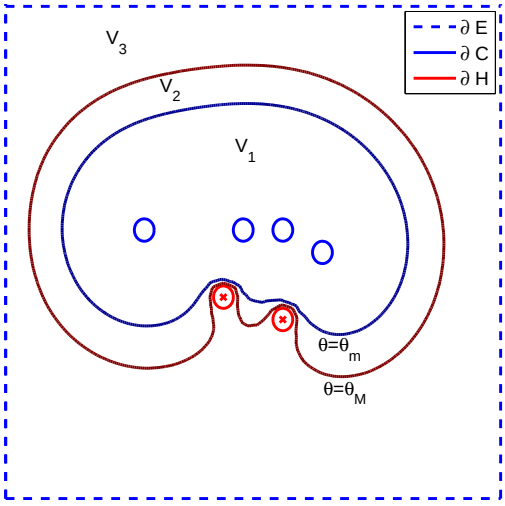

Figure 1. Scheme of a generic cryosurgery experiment: four cryoprobes (circles) and two cryoheaters (circles with crosses).

Therefore equations (1), (2) and (5) may be reformulated in the equivalent compact form

$$a(\theta)\,\frac{\partial \theta}{\partial t} = \nabla \cdot (k(\theta)\,\nabla\theta) + b(\theta) \tag{9}$$

in the fixed open volume $V = V_1 \cup V_2 \cup V_3$.

Denote by ∂C, ∂H and ∂E the union of the boundaries of all cryoprobes, all cryoheaters, and the external boundary between V and healthy tissues (see Figure 1), respectively. Boundary and initial conditions of (9) are set as

$$\begin{cases} \theta(\mathbf{x},t) = \alpha(t) & \mathbf{x} \in \partial C,\ t > 0 \\ \theta(\mathbf{x},t) = 37^o\mathrm{C} & \mathbf{x} \in \partial H \cup \partial E,\ t > 0 \\ \theta(\mathbf{x},0) = 37^o\,\mathrm{C} & \mathbf{x} \in V. \end{cases} \tag{10}$$

Here α is a given function of time expressing the decay law of the temperature of the cryoprobes: to simplify we have considered the same decay law for all cryoprobes, although the algorithm works as well if the decay law changes with the cryoprobe.

3. Numerical solution of the direct Stefan problem

The problem of finding the temperature distribution determined by a group of cold and hot cryoprobes of given positions and temperature laws is solved by an Eulero-Galerkin approach, i.e. a method combining a finite difference approximation of the time-derivative and a finite element approach solving the space dependent part of the differential problem (9)-(10).

The approximation scheme is iterative in time. If T_M is the duration of the cryosurgery experiment and $\Delta t = T_M/n$ is the time step, at each iteration $\tau = 0, 1, \ldots$ we set

$$\frac{\partial}{\partial t}\theta_{\tau+1} \approx \frac{1}{\Delta t}(\theta_{\tau+1} - \theta_\tau). \tag{11}$$

The functions a, k, and b are defined at every step of the iterative process in terms of the value of the temperature distribution at the previous step. Further comparison with (11), shows that equation (9) can be approximated by

$$\frac{a(\theta_\tau)}{\Delta t}(\theta_{\tau+1} - \theta_\tau) = \nabla \cdot (k(\theta_\tau)\nabla(\theta_{\tau+1})) + \chi(\theta_\tau)b(\theta_{\tau+1}) \tag{12}$$

where θ_τ is given and $\theta_{\tau+1}$ is the unknown. Integration of (12) against test functions $\phi \in H_0^1(V)$ and use of the Green's identity lead to the variational formulation

$$\int_V a(\theta_\tau)\,\frac{\theta_{\tau+1} - \theta_\tau}{\Delta t}\,\phi\,dv =$$

$$= \int_V [-k(\theta_\tau)\,\nabla\phi \cdot \nabla\theta_{\tau+1} + b(\theta_{\tau+1})\,\phi]\,dv. \tag{13}$$

The finite element approximation of (12) is based on (13), where boundary conditions (10) are imposed through penalization (Allaire 2007).

Given an operation time T_M, the Euler-Galerkin approach provides an approximation of the temperature distribution during the evolution from $t = 0$ to $t = T_M$. The effectiveness of the cryosurgery simulation can be quantitatively assessed by introducing a simple cost function **that counts one all defective pixels and zero all correctly treated pixels (i.e. all pixels in the tumoral region whose temperature is higher than a reference temperature and all the pixels in the healthy tissue whose temperature is smaller than this reference temperature)**. More formally, a specific configuration of the cryosurgery design is represented by a state variable $\mathbf{U}$, which is a list **set?** of N operating parameters (e.g. number and position of cryoprobes, temperature variation, etc.) whose admissible values are contained in $S \subset I\!R^N$. The cost function is the ***defect weight function*** $\mathcal{F} : S \to I\!N$ such that

$$\mathcal{F}(\theta_{\mathbf{U}}) = \int_V \mu(\theta_{\mathbf{U}}(\mathbf{x}))d\mathbf{x} \tag{14}$$

where $\theta_{\mathbf{U}}$ is the temperature distribution associated to $\mathbf{U}$ and

$$\mu(\theta(\mathbf{x})) := \begin{cases} 0 & \text{if } \theta(\mathbf{x}) < \bar{\theta} \text{ and } \mathbf{x} \text{ is diseased} \\ 1 & \text{if } \theta(\mathbf{x}) < \bar{\theta} \text{ and } \mathbf{x} \text{ is healthy} \\ 1 & \text{if } \theta(\mathbf{x}) \geq \bar{\theta} \text{ and } \mathbf{x} \text{ is diseased} \\ 0 & \text{if } \theta(\mathbf{x}) \geq \bar{\theta} \text{ and } \mathbf{x} \text{ is healthy.} \end{cases} \tag{15}$$

The most appropriate choice of the constant reference temperature $\bar{\theta}$ is discussed in (Lung et al 2004), where the defect weight function was first introduced. In our applications we have used $\bar{\theta} = -22^o$C as suggested in that paper. The cost function (14) plays a central role in the optimization procedure for the cryosurgery planning.

4. ACO optimization procedure

Ant Colony Optimization (ACO) is a statistical based optimization method developed in the nineties with the aim of providing, in a limited amount of time,

a reliable although not optimal solution to some NP-hard combinatorial optimization problems. More recently, ACO has been generalized to continuous domains (Socha and Dorigo 2003). In view of its generality and wide range of applicability, ACO has been successfully applied to a wide range of problems (e.g. (Brignone et al 2008), (Dorigo and Gambardella 1997)).

ACO takes inspiration from the way in which ants find and carry food to their nest. While an ant is going back to the nest after having taken some food, it releases a pheromone trace: this trace serves as a trail for next ants, which are able to reach food detecting pheromone. Since the pheromone decays in time, its density is higher if the path to food is shorter and more crowded; on the other hand, more pheromone attracts more ants, making longer paths to be forgotten until, at the end, all ants follow the same trail.

Ants' behavior is paraphrased in ACO identifying the cost function $\mathcal{F}$ with the length of the path to food, and the pheromone traces with a probability density which is updated at each iteration depending on the value of the cost function for a set of states. In practice, at each iteration, the cost function is evaluated on a set of P admissible states, and the states are ordered according to increasing values of the cost function. Then ACO defines a probability distribution which is more dense in correspondence of the cheaper states (i.e. the states with smallest values for $\mathcal{F}$) and, on its basis, Q new states are extracted; a comparison procedure identifies the new best P states which form the next set of states.

In more details, the starting point of the algorithm is a set of P states,

$$B := \{\mathbf{U}_k = (u_{1,k}, ..., u_{N,k}), \quad \text{such that} \\ \mathbf{U}_k \in S \subset I\!R^N,\ k = 1, \dots, P\} \tag{16}$$

that are ordered in terms of growing cost, namely, $\mathcal{F}(\theta_{\mathbf{U}_1}) \leq \cdots \leq \mathcal{F}(\theta_{\mathbf{U}_P})$.

Next, for any $j = 1, \dots, N$ e $i = 1, \dots, P$, one computes the parameters

$$m_{i,j} = u_{j,i}, \qquad s_{i,j} = \frac{\xi}{P-1} \sum_{p=1}^{P} |u_{j,p} - u_{j,i}|$$

and defines the Probability Density Function (PDF)

$$\mathcal{G}_j(t) = \sum_{i=1}^{P} w_i \mathcal{N}_{[m_{i,j}, s_{i,j}]}(t)$$

where $\mathcal{N}_{[\mu,\sigma]}(t)$ is a Gaussian function with mean value μ and standard deviation σ and

$$w_i = \mathcal{N}_{[1,qP]}(i) \tag{17}$$

with $i = 1, \dots, P$ and ξ, q real positive parameters to be fixed.

It follows that $\mathcal{G}_j$ is a superposition of normal PDFs, each one of mean $u_{j,i}$ and of variance $s_{i,j}$ proportional to the average distance between $u_{j,i}$ and the corresponding degrees of freedom of the other P configurations.

By sampling S with $\mathcal{G}_j$ Q times, the procedure generates Q new states $\mathbf{U}_{P+1}, ..., \mathbf{U}_{P+Q}$ enlarging the set B to the set of states $\tilde{B} := \{\mathbf{U}_1, ..., \mathbf{U}_{P+Q}\}$.

If $\mathbf{U}_{k_1}, ..., \mathbf{U}_{k_Q}$ are the Q states of $\tilde{B}$ of greatest cost, the updated B is defined as

$$B = \tilde{B} \setminus \{\mathbf{U}_{k_1}, ..., \mathbf{U}_{k_Q}\}.$$

This procedure converges to an optimal solution of the problem by exploiting the fact that the presence of weights w_i in the definition of $\mathcal{G}_j$ gives emphasis to solutions of lower costs since $w_1 > \cdots > w_P$. This fact, associated to the influence that a proper choice of parameters ξ and q has on the shape of the Gaussian functions, determines the way in which the method tunes the impact of the worse and best solutions.

The algorithm ends when the difference between any two states of B is less than a predefined quantity or when the maximum allowable number of iterations is reached. The initial set B of trial states is chosen by sampling a uniform probability distribution.

5. Numerical Examples

In this Section the optimization method is tested against the same $2D$ prostate phantom used in (Lung et al 2004) (see Figure 2).

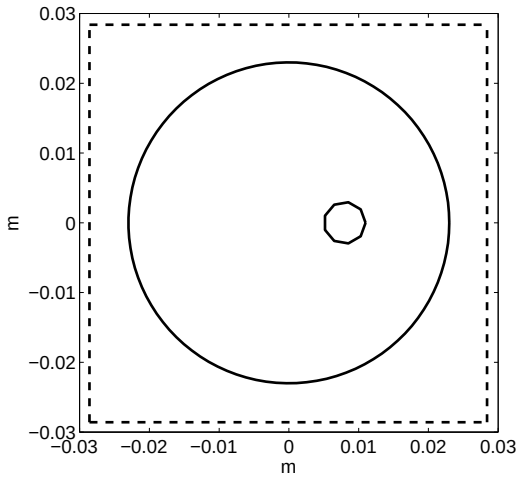

Figure 2. Prostate phantom used for numerical tests. Dashed lines delimit the area under investigation; the smallest circle inside the biggest one identify the urethra contour. **The same phantom has been used in (Lung et al 2004).**

The optimization process is performed minimizing (14) on a square containing the phantom and discretized by a grid of 1 mm x 1 mm pixels. Given a configuration of cryoprobes, the distribution of temperature is computed through the open source software FreeFem++ (Pironneau et al). The initial temperature is set to 37 ^{o}C everywhere and cryoprobes are supposed to reach -145 ^{o}C in 30 seconds; the temperature at the boundary of the urethra is set at 37 ^{o}C (see (Rabin and Stahovich 2003)) and external Dirichlet conditions are given on a square of side 0.1 m embedding the investigation domain. Phase change region V_2 is identified as the set of pixels of temperature between $\theta_m = -6$ ^{o}C and $\theta_M = 0$ ^{o}C while the threshold value $\bar{\theta}$ is -22 ^{o}C (see (Lung et al 2004)); cryoprobes as well as cryoheaters have a circular cross-section with diameter of 1 mm. The other values are chosen according to Table 1.

In the first numerical example we look for both the optimal position of a set of cryoprobes and the optimal duration of the cryosurgery experiment, (i.e. no cryoheaters are considered). Results are shown in Figures 3 - 4 and in Table 2 where the behavior of the method is tested for different numbers of cryoprobes and for different values of ACO's parameters P and Q (P is chosen as multiple of the number of probes $+1$ whereas $Q = [\frac{P}{2}]+1$ where $[\cdot]$ denotes the floor function). The value of $\mathcal{F}(\mathbf{U}_{opt})$, with $\mathbf{U}_{opt}$ optimal configurations, generally decreases as P and Q increase, although some exception to this trend can occur due to the complete randomness of the initialization of the method.

It is interesting to note that the level curve distribution in Figure 3 (c) implies a gradient of temperature from -45^oC to $+37^o$C (on the urethra boundary) over a very small distance (around 2 mm). This abrupt behavior is difficult to realize in a real experiment. However, this drawback is not due to the optimization method but to the simplistic model adopted, particularly in the definition of the boundary conditions. The aim of our paper is to assess the reliability of a novel computational approach in the case of a model widely adopted in the scientific literature. We also point out that one of the strengths of this approach is that the generalization to more realistic models is straightforward.

Parameters	Units of measurements	Values
k_1	$W/(^oC \cdot m)$	1.76
k_3	$W/(^oC \cdot m)$	0.50
$\rho_1 c_1$	$MJ/(^oC \cdot m^3)$	1.67
$\rho_3 c_3$	$MJ/(^oC \cdot m^3)$	3.35
$\rho_b w_b c_b$	$kW/(^oC \cdot m^3)$	40
q_m	kW/m^3	33.8
θ_b	^oC	37
L	MJ/m^3	300

Table 1. Model parameters used in the numerical procedure.

In the second experiment we consider the presence of cryoheaters as well as cryoprobes. Figure 5 shows the optimal solution of an experiment in which 14 cryoprobes and 3 cryoheaters have to be placed and an optimal duration has to be set: cryoprobes are constrained to fall inside the prostate, while cryoheaters are placed outside the prostate, at the same side of the urethra. Again, ACO converges to a configuration which guaranties the death of most the tumoral tissue, keeping healthy tissues over temperature $\bar{\theta}$ (the ratio between defected and total pixels is equal to 3.2% and the duration of the experiment is set by ACO to 571 seconds).

A last example shows the efficacy of our optimization method when it is applied to a more complex operation planning characterized by two distinct stages. In the first one, we want to setup the probes position; in the second one, we want to control the temperature of each cryoprobe in order that the cold front keeps on freezing the tumoral cells without invading the healthy tissue. The introduction of such a second stage is motivated by the fact that, in order to kill a tumoral cell, one has to keep its temperature low enough for an appropriate amount of time. Moreover, recent studies claimed that the killing power of cold is increased when cells are subjected to several cycles of thaw and freeze (Gage and Baust 1998) and the duration of these cycles is generally decided by medical doctors based on physiological considerations. These facts can consistently increase the duration of the operation beyond the time established by the first stage and hence a manner to control the ice propagation during the extended time becomes an essential planning

N^o cryoprobes	P	Q	Duration (sec)	Defected/Total (%)
8	27	14	1289	8.9
9	20	11	874	7.7
9	30	16	737	7.3
10	11	6	609	9.7
10	22	12	546	6.1
11	12	7	573	9.8
11	24	13	587	5.5
11	36	19	552	3.5
12	13	7	618	4.0
12	26	14	587	3.7
12 (Fig. 3)	39	20	586	1.9
13	14	8	493	5.2
13	28	15	524	2.9
14	15	8	456	5.7
14	30	16	494	3.0
15	32	17	347	2.1
15 (Fig. 4)	48	25	298	1.8
16	34	18	427	2.5

Table 2. Results for geometry of Figure 2 in the case of $q = 0.05$ and $\xi = 0.5$. Columns respectively collect the values of: number of cryoprobes, P, Q (parameters of ACO), optimal duration for the experiment and ratio between still defected area (i.e. $\mathcal{F}(\mathbf{U}_{opt})$) and investigated area.

tool.

Therefore, in more details, let us suppose that an optimal configuration of cryoprobes has been fixed in the first stage together with an optimal duration T_1. Let us further suppose that - for physiological reasons - tumoral tissues are required to maintain their temperature under the killing value $\bar{\theta}$ for a time $T_2 > T_1$. In the second stage our optimization approach is generalized to optimally determine the best temperature that each cryoprobe has to maintain in order to kill tumoral tissues and keep healthy tissues safe.

The results of this two-stage strategy are shown in Figure 6 and Table 3. Specifically, Panels (a) and (b) in Figure 6 represent the optimal positions for the 15 cryoprobes determined in stage 1 and the corresponding isotherms together with the cost function representation at $T_1 = 298$ seconds. Then, Panels (c) and (d) give the result of the second step when the cryoprobes are kept fixed and their temperatures are reported in Table 3. Finally, Panels (e) and (f) of Figure 6 show what would happen if the second stage were neglected and the cryoprobes were maintained at -145 ^{o}C up to time $T_2 = 15$ minutes.

A	1	2	3	4	5	6	7	8
B	-128	-114	-118	-134	-123	-128	-122	-112
C	-145	-145	-145	-145	-145	-145	-145	-145

A	9	10	11	12	13	14	15
B	-110	-138	-122	-128	-137	-113	-117
C	-145	-145	-145	-145	-145	-145	-145

Table 3. **Temperature optimization in a two-stage planning (second stage): the cryoprobes' configuration is in Figure 6 (c). Line A indicates the cryoprobe position (see Figure 6); line B contains the cryoprobe temperature when a second optimization stage (concerning the temperature) is applied; line C contains the cryoprobe temperature when just one optimization stage (concerning the position) is applied.**

In summary, the performances of the ACO method applied in finding the best position of the cryoprobes are nicely consistent with the state

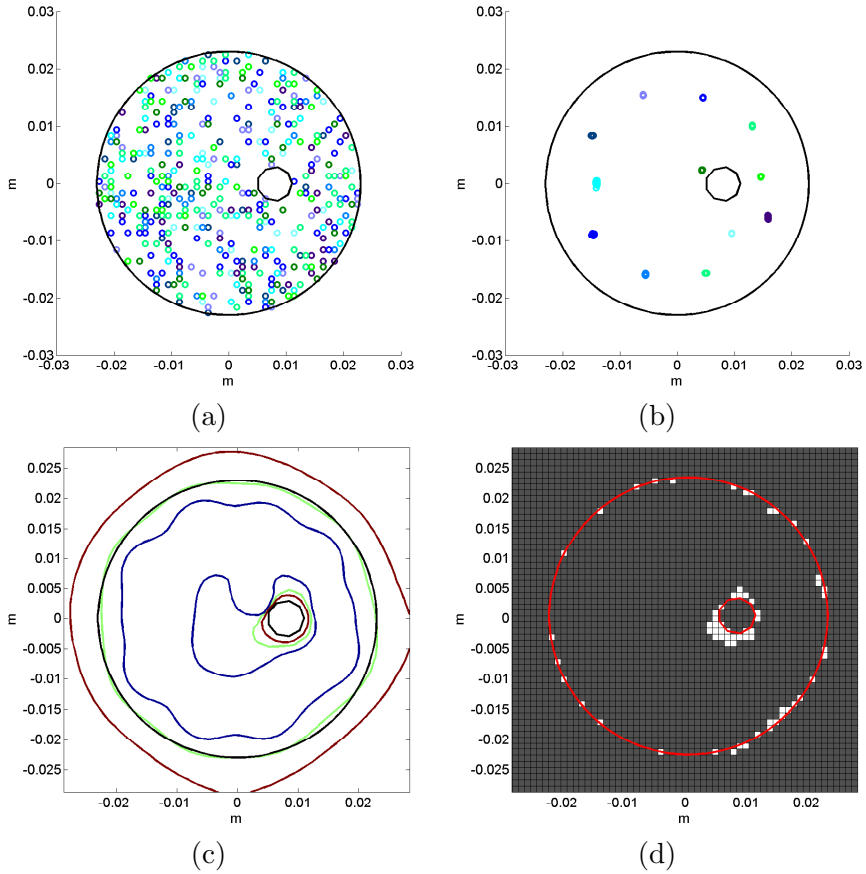

Figure 3. Case of 12 cryoprobes. (a) Initial position of $P = 39$ configurations **(where each circle represents a cryoprobe and where cryoprobes of different colors belong to different configurations)**. (b) Final position of the P configurations collapsed into one after ACO. (c) Temperature distribution for the optimal solution **(i.e. the one characterized by the minimum value of the cost function)**: 0^o C-isotherm is red, -22^o C-isotherm is green, -45^o C-isotherm is blue. (d) Plot of the defected **(i.e.** x **s.t.** $\mu(\theta(\mathbf{x})) = 1$**)** pixels (white).

of the art in cryosurgery planning and, for example, with the force-field analogy method (see (Lung et al 2004)). Further, its applicability to more general cryosurgical situations is confirmed by the good results obtained in the two-stage example showed in Figure 6 and Table 3. The computational time is of the same magnitude of most of the other optimization methods utilized in cryosurgery, although this is still far from performance requirements need by real-time operations, particularly for what concerns a 3D application of the method. In this perspective, the opportunity of integrating ACO with a geometry-based method providing some a priori uniform distribution of the cryoprobes should be considered.

6. Conclusions

In this paper we have introduced a novel optimization method for cryosurgery planning. The algorithm utilizes ACO to choose the optimal parameter configurations, where the computation of the cost function to minimize is based on the numerical solution of several direct Stefan problems. With respect to gradient-based methods, this approach can be implemented in a more straightforward way; with respect to heuristic methods, it guaranties a better flexibility and generalization power. Indeed the ACO-based method may be easily adapted to deal with

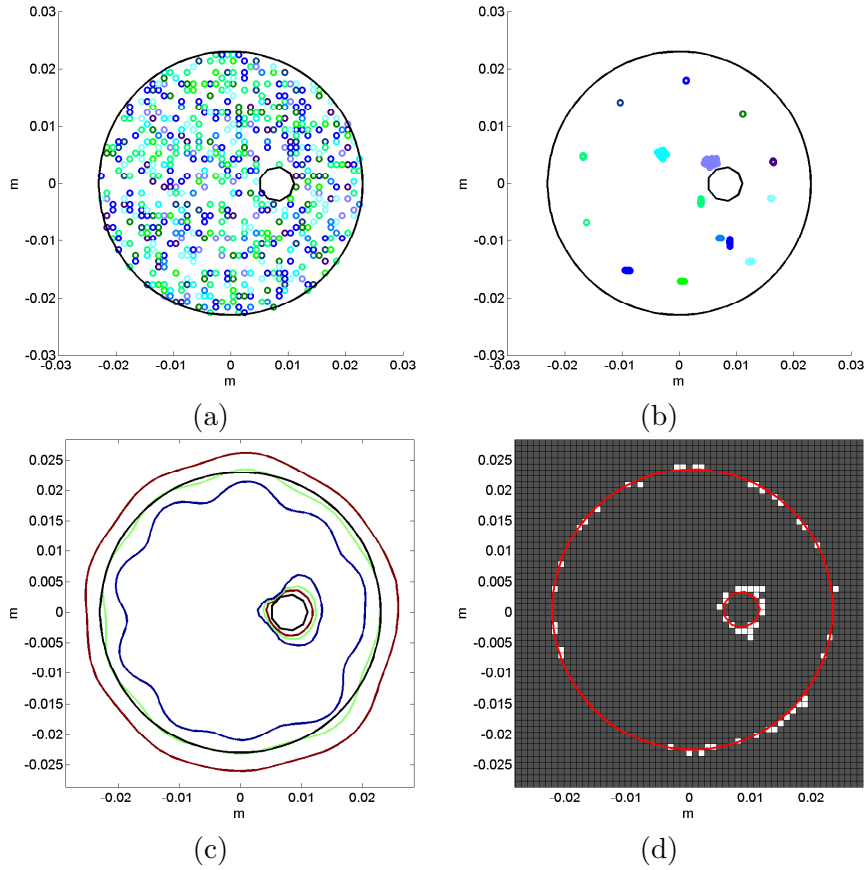

Figure 4. Case of 15 cryoprobes. (a) Initial position of $P = 48$ configurations **(where each circle represents a cryoprobe and where cryoprobes of different colors belong to different configurations)**. (b) Final position of the P configurations after ACO. (c) Temperature distribution for the optimal solution **(i.e. the one characterized by the minimum value of the cost function)**: 0^o C-isotherm is red, -22^o C-isotherm is green, -45^o C-isotherm is blue. (d) Plot of the defected **(i.e.** x **s.t.** $\mu(\theta(\mathbf{x})) = 1$**)** pixels (white).

a variety of parameters entering the numerical simulation of a cryosurgery experiment. Also, the parameters to be optimized may be divided into families to be processed in subsequent steps. Finally, if continuous functions are involved in the description of a state, they may be replaced by piecewise constant functions thus reducing the optimization problem to a finite number of degrees of freedom.

There are no a priori restrictions on the choice of the independent initial states, although common practice can suggest choices that may reduce the number of iterations. Every iteration requires the solution of several direct independent Stefan problems, but a notable saving of time may be achieved by parallelized computation that can be very naturally realized.

To simplify computations, in this paper we have been concerned with a $2D$ domain, but the approach in terms of ACO can be straightforwardly generalized to a 3-dimensional framework. Similarly, more realistic models for the direct Stefan problems can be considered where, e.g., the thermal conductivity of the solid phase depends on the temperature. Freeze-thaw processes of different cooling rates can also be considered for optimization. Also the definition of the cost function can be modified to obtain a more accurate description of defective pixels.

References

[Allaire 2007] G. Allaire, "Numerical Analysis and Optimization", *Oxford University Press*, 2007.

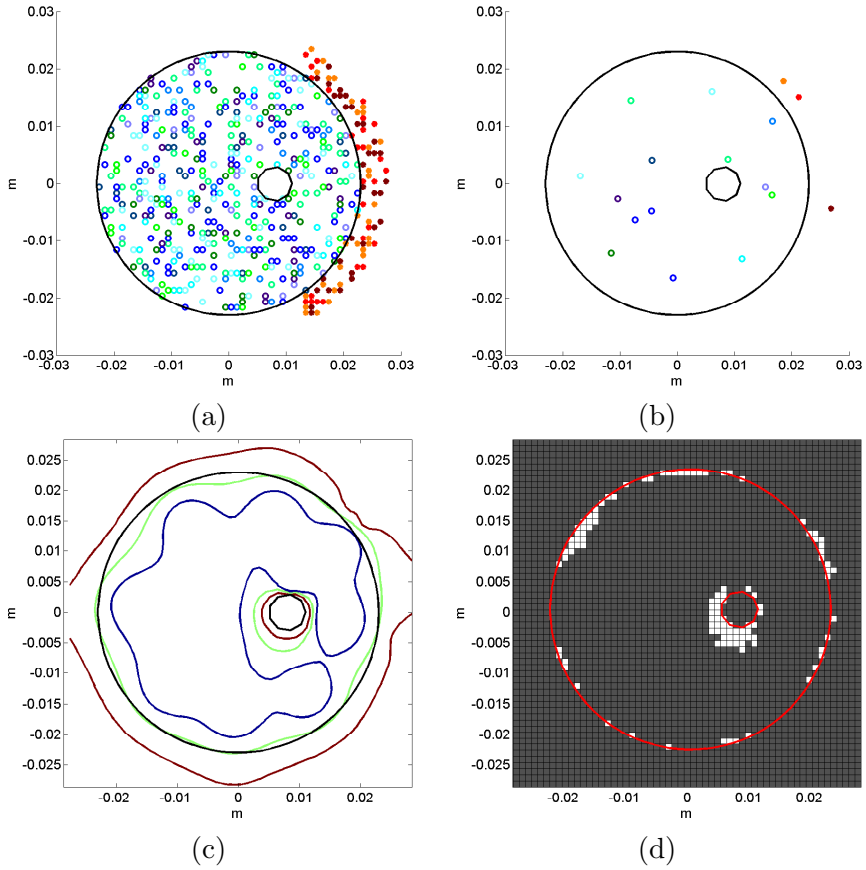

Figure 5. Case of 14 cryoprobes and 3 cryoheaters **(where each circle represents a cryoprobe and where cryoprobes of different colors belong to different configurations)**; $q = 0.015$, $\xi = 0.4$, $P = 36$, $Q = 19$. (a) Initial position of the P configurations. (b) Final position of the P configurations after ACO. (c) Temperature distribution for the optimal solution **(i.e. the one characterized by the minimum value of the cost function)**: 0^o C-isotherm is red, -22^o C-isotherm is green, -45^o C-isotherm is blue. (d) Plot of the defected **(i.e.** x **s.t.** $\mu(\theta(\mathbf{x})) = 1$**)** pixels (white).

[Bonacina et al 1973] C. Bonacina, G. Comini, A. Fasano, M. Primicerio, "Numerical solution of phase change problems", *Int. J. Heat Mass Transer* 16, pp. 1825-1832, 1973.

[Brignone et al 2008] M. Brignone, G. Bozza, A. Randazzo, M. Piana, M. Pastorino, "A Hybrid Apprach to 3D Microwave Imaging by Using Linear Sampling Method and Ant Colony Optimization", *Ieee. Trans. Ant. Prop.* 56, pp. 3224-3232, 2008.

[Baissalov et al 2000] R. Baissalov, G. A. Sandison, B. J. Donnelly, J. C. Saliken, J. G. McKinnon, K. Muldrew, J. C. Rewcastle, "A semi-empirical treatment planning model for optimization of multiprobe cryosurgery", *Phys. Med. Biol.* 45, pp. 1085-1098, 2000.

[Baissalov et al 2001] R. Baissalov, G. A. Sandison, D. Reynolds, K. Muldrew, "Simultaneous optimization of cryoprobe placement and thermal protocol for cryosurgery", *J. Water Health* 46, pp. 1799-1814, 2001.

[Cohen 2004] J. K. Cohen, "Cryosurgery of the prostate: techniques and indications", *Rev. Urol.* 6, pp. S20-S26, 2004.

[Chua and Chou 2009] K. J. Chua, S. K. Chou, "On the study of the freeze-thaw thermal process of a biological system", *Appl. Thermal Engin.* 29, pp. 3696-3709, 2009.

[Dorigo and Gambardella 1997] M. Dorigo, L. M. Gambardella, "Ant Colony System: A Cooperative Learning Approach to the Traveling Salesman Problem", *Ieee. Trans. Evol. Comp.* 1, pp. 53-66, 1997.

[Gage and Baust 1998] A. A. Gage, J. Baust, "Mechanisms of tissue injury in cryosurgery", *Cryobiology* 37, pp. 171-186, 1998.

[Keanini and Rubinsky 1992] R. G. Keanini, B. Rubinsky, "Optimization of Multiprobe Cryosurgery", *ASME J. Heat Transfer* 114, pp. 796-802, 1992.

[Lung et al 2004] D. C. Lung, T. F. Stahovic, Y. Rabin, "Computerized Planning for Multiprobe Cryosurgery using a Force-field Analogy", *Comp. Meth. in Biomech. and Biomed. Eng.* 7, pp. 101-110, 2004.

[Pennes 1948] H. H. Pennes, "Analysis of tissue and arterial blood temperature in the resting human foream", *J. Appl. Phys.* 1, pp. 93-122, 1948.

[Pironneau et al] O. Pironneau, F. Hecht, A. Le Hyaric, J. Morice, "www.freefem.org/ff++/index.htm".

[Rabin et al 2004] J. Rabin, D. C. Lung, T. F. Stahovich, "Computerized planning of cryosurgery using cryoprobes and cryoheaters", *Technology and Cancer Research & Treatment* 3, pp. 229-243, 2004.

[Rabin and Shitzer 1998] Y. Rabin, A. Shitzer, "Numerical solution of the multidimensional freezing problem during cryosurgery", *Trans. ASME* 120, pp. 32-37, 1998.

[Rabin and Stahovich 2003] Y. Rabin, T. F. Stahovich, "Cryoheater as a means of cryosurgery control",

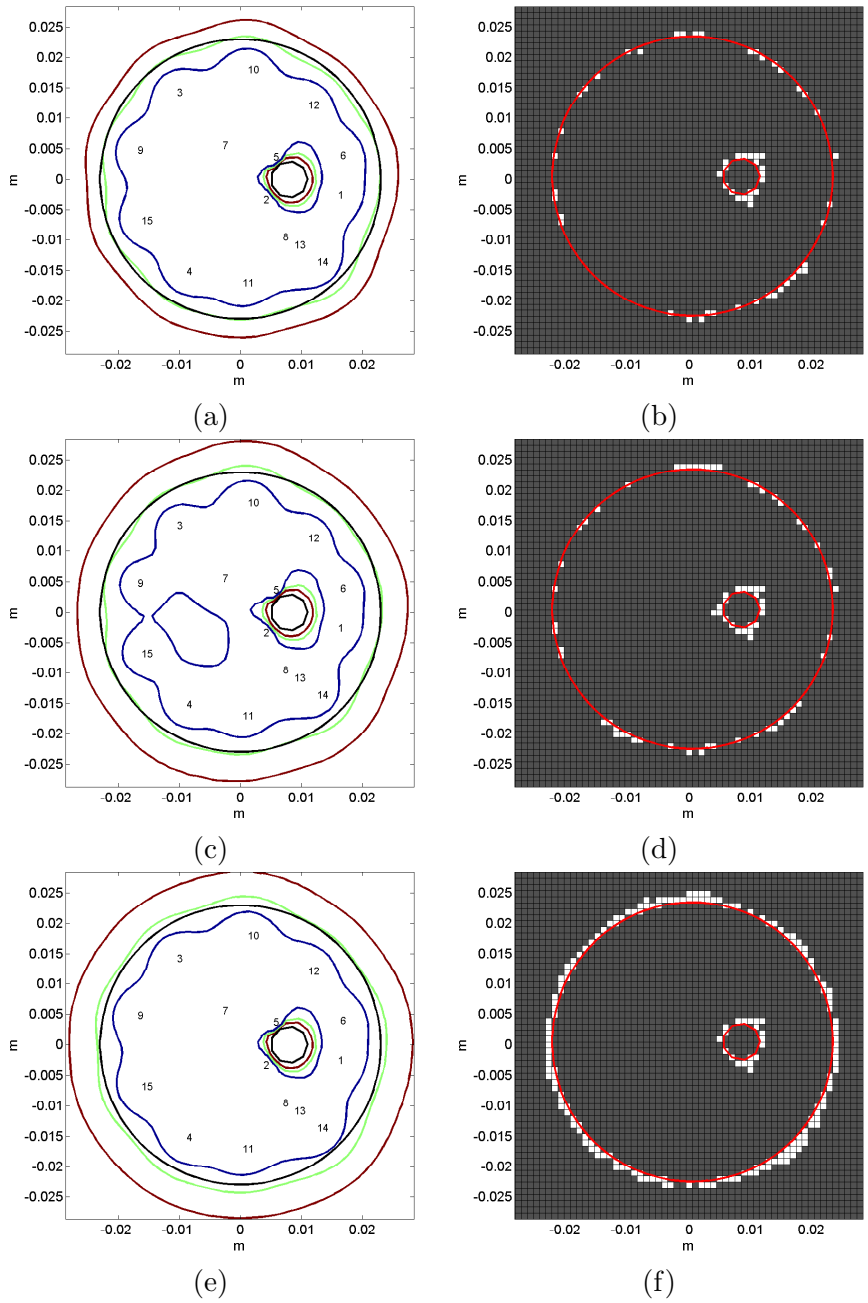

Figure 6. Two stage planning: case of 15 cryoprobes, $P = 48$, $Q = 25$, $q = 0.015$, $\xi = 0.5$. (a) and (b) contain the first stage results (see Figure 4). (c) Temperature distribution after 15 minutes with cryoprobes' temperature optimization: 0^o C-isotherm is red, -22^o C-isotherm is green, -45^o C-isotherm is blue. (d) Plot of the defected **(i.e.** x **s.t.** $\mu(\theta(\mathbf{x})) = 1$**)** pixels (white) with cryoprobes' temperature optimization. (e) Temperature distribution after 15 minutes without cryoprobes' temperature optimization: 0^o C-isotherm is red, -22^o C-isotherm is green, -45^o C-isotherm is blue. (f) Plot of the defected pixels (white) without cryoprobes' temperature optimization.

Phys. Med. Biol. 48, pp. 619-632, 2003.

[Rossi et al 2010] M. R. Rossi, D. Tanaka, K. Shimada, Y. Rabin, "Computerized planning of prostate cryosurgery using variable cryprobe insertion depth", *Cryobiology* 60, pp. 71-79, 2010.

[Rossi et al 2007] M. R. Rossi, D. Tanaka, K. Shimada, Y. Rabin, "An efficient numerical technique for bioheat simulations and its application to computerized cryosurgery planning", *Comp. Meth. Progr. Biomed.* 85, pp. 41-50, 2007.

[Rossi et al 2008] M. R. Rossi, D. Tanaka, K. Shimada, Y. Rabin, "Computerized planning of cryosurgery using bubble packing: an experimenthal validation on a phantom material", *Int. J. Heat Mass Tran.* 51, pp. 5671-5678, 2008.

[Shitzer 2011] A. Shitzer, "Cryosurgery Analysis and Experimentation of Cryoprobes in Phase Changing Media", *J. Heat Transf.* 133, pp. 011005-011017, 2011.

[Socha and Dorigo 2003] K. Socha, M. Dorigo, "Ant colony optimization for continuous domains", *Eur.*

J. Oper. Res. 50, pp. 1180 - 1189, 2003.

[Tanaka et al 2006] D. Tanaka, K. Shimada, Y. Rabin, "Two-Phase Computerized Planning of Cryosurgery Using Bubble-Packing and Force-Field Analogy", *J. Biomech. Engng.* 128, pp. 49-58, 2006.

[Theodorescu 2004] D. Theodorescu, "Cancer cryotherapy: evolution and biology", *Rev. Urol.* 6, pp. S9-S19, 2004.

[Zhang et al 2005] J. Zhang, G. A. Sandison, J. Y. Murthy, L. X. Xu, "Numerical simulation for heat transfer in prostate cancer cryosurgery", *J. Biomech. Engin.* 127, pp. 279-294, 2005.

[Zhao et al 2007] G. Zhao, H. Zhang, X. Guo, D. Luo, D. Gao, "Effect of blood flow and metabolism on multidimensional heat transfer during cryosurgery", *Med. Engng. and Phys.* 29, pp. 205-215, 2007.